Plan Irregularities Present Challenges for Seismic Design

Banikar Noman Rafiq, PG Student, MGM's College of Engineering, Nanded,

m20_banikar_noman@mgmcen.ac.in

Mohd. Zameeruddin, Associate Professor, MGM's College of Engineering, Nanded,

md_zameeruddin@mgmcen.ac.in

Abstract - In urban areas, vertical development is common in practice. Attractive elevations and smaller plan size has imposed a challenge towards the design of structural members. Especially in seismic prone zones. Indian seismic codes had provided the necessary guidelines for designing the reinforced concrete structures with different irregularities, still assessment of response is not clear. Performance based seismic design framework has provided various assessment and evaluation techniques to quantity the associative risk when subjected to seismic events. These are defined in terms of various building performance levels which is cumulative assessment of damages to structural and non-structural components. In the present study, seismic assessment of gravity based designed medium rise RC bare frames is carried out. These RC frames represent the commercial structure located in a highly seismic zone on medium soil. A parametric study has been performed to evaluate the capability of RC frames for imposed loads. In addition, damage assessment is done by using vulnerability index defined on the basis of plastic mechanism induced in the structure. The study provides a framework for assessment and evaluation of RC frames in a simplified manner.

Keywords — Structural irregularities, Performance-based seismic design, Pushover analysis, Example MRFs, Vulnerability index

I. INTRODUCTION

The devastating impacts of the global seismic events on structures have forced professional structural designers to include earthquake-resistant design onto structures for both life protection and structural functionality [Ghobarah A, 2001; Zameeruddin and Sangle, 2016]. Buildings with many stories have become more common due to the lack of available residential land and rising building costs, particularly in urban regions [Shojaei, F., & Behnam, B. 2017]. The manner in which a medium-rise building responds to seismic loads is determined by its structural design [Moehle, J. P., 2006]. The primary causes of structural failures during seismic events are irregular structural arrangements, either in plan or elevation. The inelastic behavior of reinforced concrete components subjected to inelastic aggression cannot be addressed by the earthquake resistant design approaches outlined in the current seismic codes [De Luca, F., & Verderame, G.M. 2015]. In order to address inelastic invasion, these codes offer an indirect method of applying a modification factor to the strength and displacements [Mondal et al., 2013]. The Performance-based Seismic Design (PBSD) documents' predictive design approach turned out to be the most effective substitute for the seismic-code based methods [FEMA 445, 2005; Zameeruddin and Sangle, 2021]. The nonlinear static or nonlinear dynamic analysis processes serve as the foundation for the performance evaluation procedures outlined in PBSD publications. The nonlinear static methods are becoming more popular among engineers in practice because of how simple they are to use. The displacement coefficient method (DCM) and the capacity spectrum method (CSM) are two performance evaluation techniques based on the nonlinear static method [ATC 40, 1996; FEMA 273, 1996; FEMA 356, 2000; ASCE/SEI 41, 2007; Zameeruddin and Sangle, 2021; Boroujeni ARK 2013]. In PBSD, the structural performance is assessed based on the damages incurred by the structural and non-structural components [Couto, R., Sousa, I., Bento, R., Castro, J.M., 2022]. Operational levels, immediate occupancy, life safety range, and collapse prevention are the names given to these performance levels [Padalu, P.K.V.R., & Surana, M., 2024]. The collapse mechanisms that emerge from the performance analysis demonstrate the yielding of structural elements but are unable to calculate damage [V. M. Mokashi et al. 2024]. An evaluation of the performance of modelled moment resisting frames (MRFs) with plan irregular geometries under lateral load patterns as outlined in IS 1893 [2016] has been performed in this study. Parametric investigations on the fundamental period, roof displacement, inter-story drift ratio, and base shear are included in the performance assessment. In addition, the

 DOI : 10.35291/2454-9150.2024.0358

study utilizes the Pushover Analysis (POA) results in an attempt to correlate the global damage value with the building performance levels as defined in PBSD.

II. STRUCTURAL IRREGULARITIES

In metropolitan locations, medium-rise building construction is recommended to reduce the requirement for affordable housing. Uneven structural configuration has become a routine procedure for medium-rise buildings in order to achieve the minimal requirements for the floor space ratio. As a result, structures were built with uneven mass, stiffness, and strength distributions along the building's plan and height [Bhosale et al., 2017; Soni and Mistry, 2006].

Several plan and elevation irregularities have been documented in IS 1893:2016. These irregularities fall into two categories: Plan and vertical. All of these categories are presented in Table 1. The current study examines inconsistencies in plans for medium-rise structures. In the construction of medium-rise structures, five types of plan irregularities are typically used. These consist of non-parallel lateral force systems, torsional irregularity, re-entrant corners, floor slabs with excessive cut-outs or openings, and out-of-plane offsets in vertical elements. As per IS 1893:2016, Figure 1 depicts the irregularity in the plan.

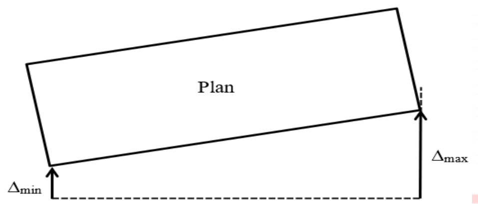

1(a). Torsional Irregularity $\Delta_{max} = 1.5\ \Delta_{min}$

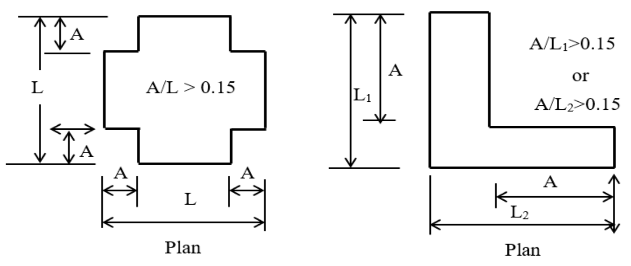

1(b) Re-entrant Corners

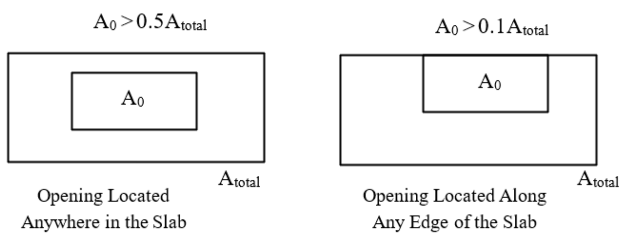

1(c) Floor Slabs having Excessive Cut-outs or Openings

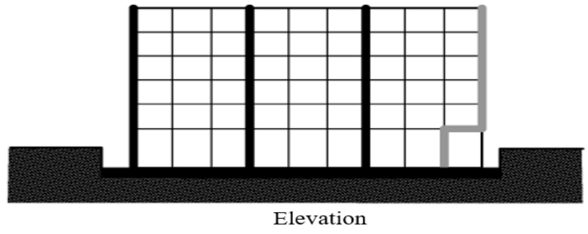

1(d) Out of plane offsets in vertical elements

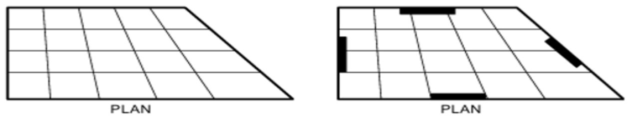

1(e) Non-parallel lateral force system

Fig 1: Various Plan Irregularities

The performance of torsional irregular and re-entrant corner structures has been assessed in this study.

Table 1: Various plan irregularities

Type of Irregularity	Definition	IS 1893-2016 Section No.
Torsional Irregularity	When the ratio of maximum horizontal displacement at one end and the minimum horizontal displacement at the other end is in the range of 1.5 – 2.	Clause No. 7; recommendation - the building configuration shall be revised.
Re-entrant Corners	When the structural configuration in plan has a projection of size greater than 15 percent of its overall plan dimension in that direction	Clause No. 7; recommendation – 3D dynamic Analysis
Floor Slabs having Excessive Cut-outs or openings	When floor slabs have cut-outs or openings of area is more than 50 percent of the full area of the floor slab.	Clause No. 7; recommendation – (a) opening less than 50 %, the floor slab shall be taken as rigid or flexible and (b) if openings are more than 50 %, the floor slab shall be taken as flexible.
Out-of-Plane Offsets in Vertical Elements	Out-of-Plane Offsets in vertical elements resisting lateral loads cause discontinuities and detours in the load path, which is known to be detrimental to the earthquake safety.	Clause No. 7; recommendation – (a) IS 1893 and IS 13920 recommendations shall be strictly followed, (b) Lateral drift shall be less than 0.2 % in the storey having the offset and, in the storeys, below.
Non-parallel Lateral Force System	Lateral force resisting system oriented along two plan directions that are orthogonal to each other.	Clause No. 7; recommendation – buildings shall be analyzed for load possible combinations of three components of earthquake EL_x, El_y and EL_z

III. PERFORMANCE-BASED SEISMIC DESIGN

PBSD is a comprehensive approach that employs performance evaluation methodologies and accurate nonlinear modeling tools to ensure that structures can withstand seismic forces [Performance-Based Seismic Design for Tall Buildings by the Council on Tall Buildings and Urban Habitat (CTBUH), 2017]. Nonlinear static and

 DOI : 10.35291/2454-9150.2024.0358

dynamic analysis techniques have been included in PBSD; nevertheless, nonlinear static techniques are frequently chosen because of their simplicity and accessibility [Kuria et al., 2024]. The displacement coefficient method (DCM) and the capacity spectrum method (CSM) are the two nonlinear static methods mentioned in PBSD. CSM compares the capacity of the structure (capacity spectrum) with the demands of the structure (demand spectrum).

Figure 2 shows how the performance point is determined in seismic analysis according to the ATC 40 guidelines. The capacity spectrum depicts the building's resistance to lateral forces, while the elastic demand spectrum represents the expected demand due to earthquake loading. The reduced demand spectrum reflects inelastic behavior, intersecting the capacity spectrum at the performance point. This point marks the structure's anticipated response level during seismic events, balancing its capacity and the expected demand.

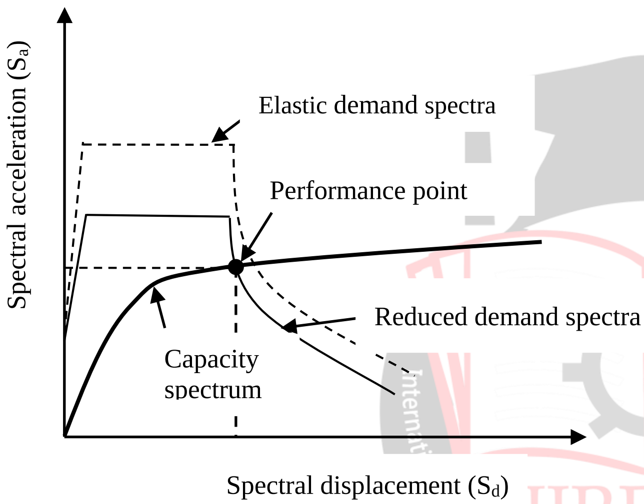

Fig. 2. Determination of performance point as per ATC-40

The Displacement Coefficient Method (DCM) provides a simple way to estimate target displacement, which is the expected roof displacement of a structure during a seismic event. This method avoids the need for converting the capacity curve into spectral coordinates [AL-Saedi, M.A.H., & Yaghmaei-Sabegh, S., 2024; Baltzopoulos, G., Chioccarelli, E., & Iervolino, I., 2015]. As shown in Fig. 3, the capacity curve represents the relationship between base shear and roof displacement, marking key points like Initial Stiffness K_i, Yield Base Shear V_y, Effective Stiffness K_e, and Post-Yield Stiffness αK_e, The Target Displacement δ_t is derived from this curve, allowing for an efficient seismic performance assessment.

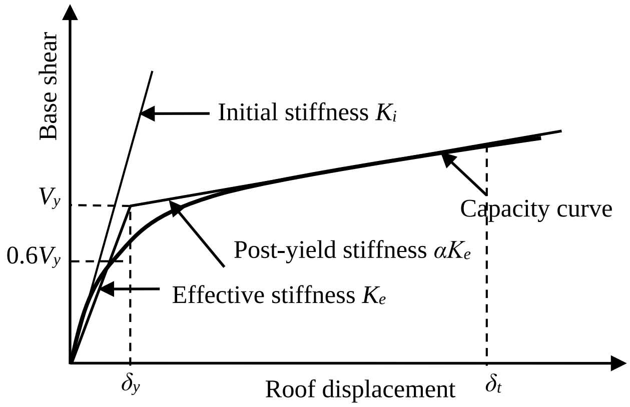

Fig. 3. Calculation of target displacement

These techniques are effective at finding collapse mechanisms and anticipating nonlinear responses, but they don't accurately quantify the corresponding damage level [Chaudhary, S., & Choudhury, S., 2022]. The present research focuses on finding engineering demand parameters that are correlated with structural loss or damage in order to mitigate this limitation. This method aims to offer designers a more rational and predictive tool for damage state assessment in the design phase.

When medium-rise buildings are situated in an area with high seismic activity, evaluating their seismic performance becomes more difficult [Jia et al., 2022]. Table 2 enumerates the quantitative performance evaluation techniques suggested by current codes of practice [Boroujeni ARK 2013]. The majority of seismic codes recommend using dynamic analysis—which may make use of elastic response spectrum analysis or elastic time history—to estimate the lateral load distribution over the structure [Jain, S.K., 2016]. It is not preferred in typical design practice to do a dynamic analysis to understand the nonlinear response of the structure because it is a complicated task [Kuria et al. 2024]. Since non-linear static methods (NLSP) are the most straightforward, they are frequently used in design practice [Bento et al., 2004].

Table 2: Various analysis procedures to estimate seismic responses

Type of Analysis	Usual Name	Dynamic effects	Material non-linearity
Linear static	Equivalent static	No	No
Linear dynamic	Response spectrum	Yes	No
Nonlinear static	Pushover	No	Yes
Nonlinear dynamic	Time history	Yes	Yes

IV. PUSHOVER ANALYSIS

Pushover Analysis (POA) procedure consists of applying a vertical distribution of lateral loads to a model which captures the material non – linearity's of an existing or previously designed structure, and monotonically increasing those loads until the peak response of the structure is

 DOI : 10.35291/2454-9150.2024.0358

ISSN : 2454-9150 Vol-10, Issue-07, Oct 2024

obtained on a base shear vs. roof displacement plot as shown in figure 4, this allows the deformation of structural member (e.g. Plastic-hinge sequence) [Marcelo et al., 2021].

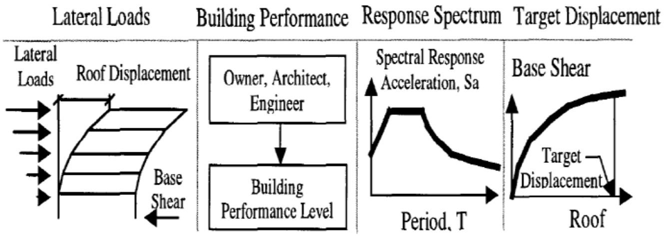

Fig.4 POA Procedure

The inelastic modelling of reinforced concrete members impacts the accuracy of POA. By assigning the plastic hinges, the inelastic characteristics of the reinforced concrete components are introduced. PBSD has put forth two actions of plastic hinges viz. deformation-controlled (ductile action) or force-controlled (brittle action) [Bajaj et al., 2024]. The inelastic force-deformation curve Fig. 5(a) demonstrates how a structure responds as lateral loads increase. Key deformation stages are highlighted, such as Immediate Occupancy (IO), Life Safety (LS), and Collapse Prevention (CP), each reflecting a specific level of performance. These stages illustrate the shift from initial elastic behavior (segment AB) to inelastic deformation (segment BC), eventually reaching post-yield degradation (segment CD). Points "a," "b," and "c" mark distinct resilience thresholds, outlining critical ranges where managing structural damage is essential. This model provides an effective way to predict flexural failure during pushover analysis, capturing both ductile and brittle phases of the structural response .In the present study the effects of axial force on beams were disregarded, considering the presence of rigid diaphragms. However, these effects were considered for the columns. Fig. 5 and Table 3 gives details of plastic rotation limits for reinforced concrete beams and columns described in PBSE documents.

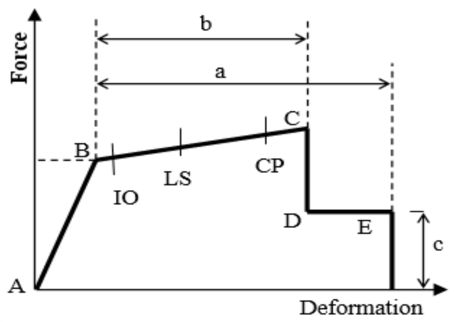

(a) Deformation control (flexure failure)

In order to identify locations that are likely to exceed the elastic range under seismic stress, plastic hinges were placed in the pushover analysis according to the configuration depicted in Fig. 5(b), with P-M3 hinges at column ends and M3 hinges at beam ends. In accordance with the concepts of Performance-Based Seismic Design (PBSD), this hinge configuration efficiently simulates flexural response and possible failure zones. Rotation limits for evaluating RC beams and columns are given in Tables 3 and 4, and the hinge characteristics adhere to FEMA 356 criteria.

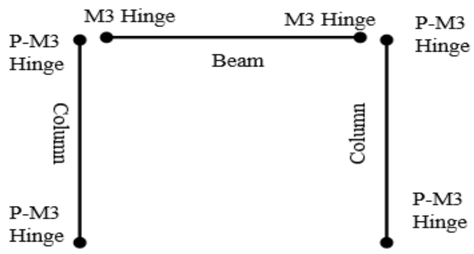

(b) Location of hinges

Fig. 5: Idealized inelastic force–deformation relationship

In Stage I, gravity loads were applied as the distributed element loads on the basis of the yield line theory and concentrated loads from secondary beams. Gravity analysis was performed for full gravity load in a single step (i.e., force-control). The state of the structure in this analysis was saved and was subsequently recalled in Stage II. In Stage II, lateral loads were applied monotonically in a step by-step nonlinear static analysis.

Table 3: Plastic rotation limits for RC beams controlled by flexure [FEMA 356]

Conditions			Modelling Parameters			Acceptance Criteria				
			Plastic rotation angle (radians)		Residual strength ratio	Plastic rotation angle (radians)				
						Performance level				
$\frac{P}{A_g f_c'}$	Trans. Reinf.	$\frac{V}{b_w d \sqrt{f_c'}}$				IO	Component type			
							Primary		Secondary	
			a	b	c		LS	CP	LS	CP
≤ 0.5	C	≤ 3	0.02	0.03	0.2	0.005	0.010	0.02	0.02	0.03

C indicates the transverse reinforcement meets the criteria for ductile detailing

Table 4: Plastic rotation limits for RC columns controlled by flexure (FEMA 356)

Conditions			Modelling Parameters			Acceptance Criteria				
			Plastic rotation angle (radians)		Residual strength ratio	Plastic rotation angle (radians)				
						Performance level				
$\frac{\rho - \rho'}{\rho_{bal}}$	Trans. Reinf..	$\frac{V}{b_w d \sqrt{f_c'}}$				IO	Component type			
							Primary		Secondary	
			a	b	c		LS	CP	LS	CP
≥ 0.1	C	≤ 3	0.02	0.03	0.2	0.005	0.015	0.02	0.02	0.03

C indicates the transverse reinforcement meets the criteria for ductile detailing

Because the lateral force profile in pushover analysis influences the structural response. IS1893:2016 trivial lateral load patterns were applied.

V. EXAMPLE MRFs

The example MRFs considered for this study represents regular and irregular frames (with plan irregularities). The Plan irregularities is introduced in the MRFs in accordance to the guidelines of IS 1893:2016. Table 5 provides the details of example MRFs. These MRFs are considered to be bare frames located in the zone V (zone factor, 0.36) which is the severest zone as per IS 1893 and soil type is medium. The structure importance factor used is 1.0. The modification factor of 5 was used to account for the ductility in MRFs.

Table 5: Details of example MRFs used in the study

Frames	Height (m)	T_d (s)	W_i (kN)	A_h	Vd (kN)
S7B3	21	1.106	22842.94	0.06	1010.7
S7B3-14H	21	1.092	20664.58	0.06	926.11

DOI : 10.35291/2454-9150.2024.0358

S7B3-28H	21	1.174	22043.85	0.06	919.15
S7B3-42H	21	1.064	16307.87	0.06	750.10

**S represents storey, B represents bays, H represent horizontal direction and number says about percentage reduction in plan areas.

Fig. 6 shows the typical layout of the example MRFs. Four different types of plan irregularities have been considered in the present work which, are commonly found in urban constructions in India. Plan irregularity introduced represents re-entrant corners and torsional irregularities of 14, 28, 42 and 56 percent of the plan width of the structure. Similar regular building having no unusual irregularity in spatial form have been studied to benchmark the results of the parametric studies. For the analysis, the dead loads, live (imposed) loads, and seismic loads on example MRFs were considered as per IS 875 (Part 1 and 2) [1987] and IS 1893 [2016], respectively. These example MRFs are subjected to the mean dead load of 45 kN/m (inclusive of the finishes loads) and mean live load of 15 kN/m for all floors. The design of reinforced concrete sections is done following the guidelines of IS 456 and their detailing is done as per IS 13920 specifications. Table 6 provides the material properties and design constants used in the design. Table 7 shows the design details of the reinforced concrete sections. The structural design of the example MRFs is not a unique solution available for the calculated demand. Based on the same demand, different designers may select different solutions. The RC member sizes were selected by following a common practice adopted by professional engineers.

Table 6: Material properties considered in the design of example MRF [IS456, IS1786]

Material property	Concrete M 25 Grade	Steel Fe 415 grade
Weight per unit volume (kN/m^3)	25	76.97
Mass per unit volume (kN/m^3)	2.548	7.849
Modulus of elasticity (kN/m^2)	27.3E+06	2E+08
Characteristic strength (kN/m^2)	30000 (for 28 days)	415000 (yield)
Minimum tensile strength (kN/m^2)	-	485800
Expected yield strength (kN/m^2)	-	456500
Expected tensile strength(kN/m^2)	-	533500

All the columns and beams in a selected story are identical in cross section. The column remained uniform in cross section up to two or three stories, depending on the height of the building. Table 8 describes the modal analysis results of example MRFs.

Table 7: Summary of structural design for example MRFs

Example MRFs	Storey No	External/Internal Column size (mm)	External/Internal Column Rebar's (mm^2)	Beams size (mm)	Beams Top Rebar's (mm^2)	Beams Bottom Rebar's (mm^2)
S7B3	1-4	(CE1) 450×450	3484	(B1) 380×380	1896	948
		(CI1) 530×530	4221			
	5-7	(CE2) 380×380	1155	(B2) 300×300	1529	1016
		(CI2) 450×450	1672			
S7B3-14H	1-4	(CE1) 450×450	3465	(B1) 380×380	1957	978
		(CI1) 530×530	4046			
	5-7	(CE2) 380×380	1155	(B2) 300×300	1622	1148
		(CI2) 450×450	1734			
S7B3-28H	1-4	(CE1) 450×450	3461	(B1) 380×380	2104	1052
		(CI1) 530×530	3461			
	5-7	(CE2) 380×380	1223	(B2) 300×300	1743	1320
		(CI2) 450×450	1844			
S7B3-42H	5-7	(CE1) 450×450	2993	(B1) 380×380	1971	985
		(CI1) 530×530	3504			
	1-4	(CE2) 380×380	1155	(B2) 300×300	1674	1222
		(CI2) 450×450	1717			
S7B3-56H	1-4	(CE1) 450×450	1730	(B1) 380×380	1955	977
		(CI1) 530×530	3710			
	5-7	(CE2) 380×380	1157	(B2) 300×300	1629	1157
		(CI2) 450×450	1779			

Table 5 displays the natural period of vibration, for example, MRFs calculated using the empirical equation provided in IS 1893:2016 for buildings without infills. Additionally, modal analysis of the example MRFs has been carried out to determine the Eigen value-based fundamental period of vibration; its results are documented in Table 8. It is not a unique solution, but rather an identified rational approach to the problem. It finds out that the values derived from the code empirical relation are shorter than the fundamental period obtained using the Eigen value analysis.

The variations in the cross-sectional areas of RC members and the span of a building's member, which are not taken into consideration by the IS a code empirical

 DOI : 10.35291/2454-9150.2024.0358

ISSN : 2454-9150 Vol-10, Issue-07, Oct 2024

relationship, can be attributed for the discrepancy in the vibration time period (given in Table 9). Modal mass participating ratio shown in Table 10 illustrates the correlation between higher mode participation and irregularity.

Table 8 (a): Modal analysis results of S7B3 MRFs

Storey Level	S7B3			
	Modal time Period (T_m)	Modal Frequency (ω_m) cycles/sec	Stiffness (kN/mm)	Lateral Loads (kN)
1	1	1.10	0.90	32.24
2	2	1.10	0.90	32.24
3	3	0.99	1.00	39.84
4	4	0.40	2.49	246.15
5	5	0.40	2.49	246.15
6	6	0.37	2.66	281.12
7	7	0.21	4.68	867.44

Using SAP2000 v20, the POA was carried out on the example MRFs for lateral load distribution, which was obtained with reference to IS 1893:2016 recommendations. The pushover curves, which are usually the base force vs. roof displacement plot, are used to showcase the POA results.

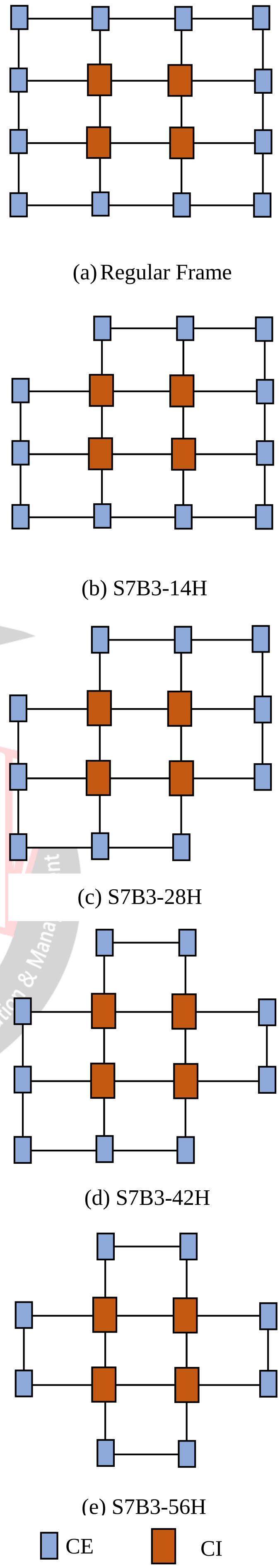

Fig. 6: Typical layout of Example MRFs

 DOI : 10.35291/2454-9150.2024.0358

ISSN : 2454-9150 Vol-10, Issue-07, Oct 2024

Table 8 (b): Modal analysis results of S7B3-14H MRFs

Storey Level	S7B3-14H			
	Modal time Period (T_m)	Modal Frequency (ω_m) cycles/sec	Stiffness (kN/mm)	Lateral Loads (kN)
1	1.10	0.90	32.61	123.62
2	1.09	0.91	33.07	311.01
3	0.98	1.01	40.90	215.98
4	0.39	2.52	252.37	143.21
5	0.39	2.53	252.89	81.43
6	0.36	2.72	293.24	36.19
7	0.21	4.75	891.58	9.04

Table 8 (c): Modal analysis results of S7B3-28H MRFs

Storey Level	S7B3-28H			
	Modal time Period (T_m)	Modal Frequency (ω_m) cycles/sec	Stiffness (kN/mm)	Lateral Loads (kN)
1	1.19	0.83	27.69	143.52
2	1.17	0.85	28.63	295.82
3	1.05	0.94	35.15	205.43
4	0.42	2.32	214.07	139.86
5	0.42	2.34	216.77	80.19
6	0.39	2.51	250.32	35.64
7	0.22	4.41	770.88	8.91

Table 8 (d): Modal analysis results of S7B3-42H MRFs

Storey Level	S7B3-42H			
	Modal time Period (T_m)	Modal Frequency (ω_m) cycles/sec	Stiffness (kN/mm)	Lateral Loads (kN)
1	1.07	0.92	34.14	97.81
2	1.06	0.93	34.84	252.44
3	0.94	1.05	44.17	175.30
4	0.38	2.61	269.31	116.40
5	0.37	2.63	273.46	66.27
6	0.34	2.89	331.88	29.45
7	0.20	4.95	968.99	7.36

Table 8(d): Modal analysis results of S7B3-56H MRFs

Storey Level	S7B3-56H			
	Modal time Period (T_m)	Modal Frequency (ω_m) cycles/sec	Stiffness (kN/mm)	Lateral Loads (kN)
1	1.14	0.87	29.97	108.54
2	1.14	0.87	29.97	232.06
3	1.00	0.99	38.98	161.15
4	0.40	2.44	236.21	110.05
5	0.40	2.44	236.21	63.26
6	0.36	2.73	295.27	28.11
7	0.21	4.68	867.52	7.03

The example MRFs' pushover curves are shown in Fig. 7. The performance point is located at the intersection of the capacity curve and the inelastic demand spectra.

Table 9: Modal Analysis results of the example MRFs

Example MRF	T_m	T_d	Difference (%) = $[T_m-T_d/T_d]$x100
S7B3	1.10	0.73	50.54
S7B3-14H	1.10	0.73	49.69
S7B3-28H	1.19	0.73	62.45
S7B3-42H	1.07	0.73	46.30
S7B3-56H	1.14	0.73	56.15

Table 10: Modal Participation factors of the example MRFs

Example MRF	Mode1	Mode 2	Mode 3
S7B3	99.79	99.83	3.41E-13
S7B3-14H	99.80	99.80	0.0631.73
S7B3-28H	99.81	99.81	1.10E-14
S7B3-42H	99.81	99.81	0.1041
S7B3-56H	99.70	99.92	1.39E-14

Table 11: Base force and displacement at performance point for various PBSE methods

PBSE Methods	ATC 40 (CSM)		FEMA 356 (DCM)	
Model	**V_p, (kN)**	**d_p, (m)**	**V_p, (kN)**	**d_p, (m)**
S7B3	2467.61	0.18	2905.22	0.251
S7B3-14H	2225.62	0.18	2607.67	0.249
S7B3-28H	2088.68	0.20	2377.46	0.267
S7B3-42H	1864.84	0.20	2022.01	0.243
S7B3-56H	1766.66	0.22	2170.64	0.319

The values of the base force and displacement obtained at the performance point for various types of PBSE techniques applied to model MRFs are provided in Table 11. The values of the roof displacement obtained from various PBSE methods showed that the displacement of S7B3-56H MRF with plan irregularity is largest one compare to other type of example irregular MRFs.

VI. Results and Discussions

The example MRFs' collapse mechanism is shown in Fig. 7. The mechanism illustrates formation of plastic hinges and attainment of different performance levels. These performance levels are referred to as Operational (OP), Immediate Occupancy (IO), Life Safety range (LS), Collapse Prevention (CP), and Collapse (C). The building performance is evaluated on the basis of damages to structural and non-structural components. The damage attainment is classified in three levels, viz; (a) associated repairs, (b) associated downtime and (c) associated casualties. Indian seismic code provision addresses the first level of damage attainment. PBSD helps to overcome this limitation.

In PBSD the capacity of the structure is assessed on the basis of nonlinear responses at performance point, which is typical intersection of capacity spectrum and demand

 DOI : 10.35291/2454-9150.2024.0358

spectrum. The performance levels may be obtained by two different methods; CSM and DCM. The obtained results are in line with the results obtained from time history analysis.

The simple measure of inelastic behaviour is drift or displacement attained at critical locations. Fig. 7 shows the storey displacement and inter-storey drift of all example MRFs.

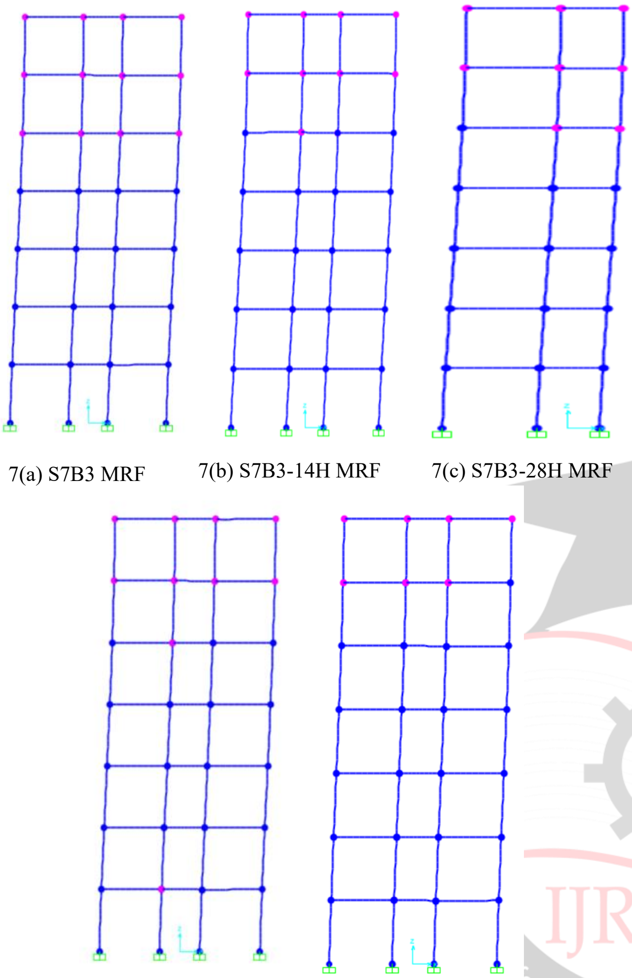

7(a) S7B3 MRF 7(b) S7B3-14H MRF 7(c) S7B3-28H MRF

7(d) S7B3-42H MRF 7(e) S7B3-56H MRF

Fig. 7: Collapse mechanism of Example MRFs

VII. Vulnerability Index

In present study the scaling of damage to structural component is done in a range of 0 to 1. “0” indicates no damage and “1” shows the complete collapse. Intermediate values illustrate acceptable level of risk. The limit state of risk attributes towards loss of ductility, strength and stiffness. In past several attempts have been made to quantify these losses. The present work provides simple method of quantifying the damage values through the counts of plastic hinges at a considered performance level. The following expression shows the formulation for the proposed damage level.

$$VI = \frac{\sum H_B}{\sum H_B + \sum H_C}$$

Where,

VI = Vulnerability Index

$\sum H_B$ = Hinges formed in beams members at performance point.

$\sum H_C$ =Hinges formed in column members at performance point

Table 12 shows the VI values of all example MRFS

Table 12: VI values of all example MRFS

Example Frame	P-M2-M3 Hinges	M3 Hinges	Overall Hinges	VI
S7B3	224	336	560	0.4
S7-B3-14H	210	308	518	0.405
S7-B3-28H	199	280	479	0.415
S7-B3-42H	185	252	437	0.423
S7-B3-52H	171	224	395	0.432

Seismic design of a medium and high-rise structure with plan irregularity imposes different challenges. These includes maintaining the ductility, avoiding torsional effects, maintaining the strength loss and unequal stiffness distribution. Present study proposed different way of introducing the plan irregularities to cater with these problems. When subjected to seismic hazard these buildings are subjected to inelastic incursions, raising the threat to structure and life. Using PBSD, it's easy to attain the peak value of nonlinear responses, but the damage state remains unanswered. An attempt has been made to evaluate or identify the damage level by introducing a vulnerability index. This is not a unique solution but rather a rational approach to addressing the problem.

VIII. Conclusion

This study evaluated the impact of plan area reduction on structural performance, using the Vulnerability Index (VI) to gauge seismic damage susceptibility. The reduction in plan area significantly increased the VI, with S7B3-56H showing the highest vulnerability in the CP range. This indicates the negative impact of irregularity on seismic resilience, highlighting concentrated stress and earlier plastic hinge formation. The pushover analysis provided insights into inelastic drift attainment, with hinges serving as indicators of structural damage.

The study's methodology offers a rational approach to quantifying structural damage due to geometric irregularities, providing a framework for evaluation not defined in standard PBSD documents. This approach could efficiently assess structural damage states, contributing to improved seismic design practices in high-risk zones.

Acknowledgment

The authors of this paper acknowledge the research contributions of all the citations under reference. The support provided by the Chairman and Director, Mahatma Gandhi Missions College of Engineering, Nanded is highly respected.

References

[1] Al-Saedi, M.a.h., & Yaghmaei-Sabegh, S. (2024). Seismic Vulnerability Assessment of Regular and

 DOI : 10.35291/2454-9150.2024.0358

Irregular Reinforced Concrete Shear Wall Buildings Using Fragility Curves.Iran J Sci Technol Trans Civ Eng. https://doi.org/10.1007/s40996-024-01435-4

[2] ASCE/SEI 41. (2007). American Society of Civil Engineers. Seismic rehabilitation of existing building. Reston, Virginia.

[3] ATC-40. (1996). Seismic evaluation and retrofit of existing concrete buildings. Redwood City (CA): Applied Technical Council.

[4] Bajaj, R., & Yadav, S. (2024). Estimation of elastic and inelastic seismic behavior of reinforced concrete framed structures. Asian J Civ Eng, 25, 1613–1624. https://doi.org/10.1007/s42107-023-00866-0

[5] Baltzopoulos, G., Chioccarelli, E., & Iervolino, I. (2015). "The Displacement Coefficient Method in Near-Source Conditions". Earthquake Engineering & Structural Dynamics, 44(10), 1627-1641. https://doi.org/10.1002/eqe.2497

[6] Bento, R., Falcão, S., & Rodrigues, F. (2004). Non-Linear Static Procedures in Performance Based Seismic Design. 13th World Conference on Earthquake Engineering. Vancouver, B.C., Canada. Paper No. 2522.

[7] Bento, R., Falcão, S., & Rodrigues, F. (2004). Non-Linear Static Procedures in Performance-Based Seismic Design. 13th World Conference on Earthquake Engineering (pp. 1-8). Vancouver, B.C., Canada. https://doi.org/10.3233/978-1-60750-159-5-2522

[8] Bhosale, A. S., Davis, R., & Sarkar, P. (2017). ASCE-ASME. J. Risk Uncertainty Eng. Syst. Part A: Civ. Eng., 03(3): 04017001-10. https://doi.org/10.1061/AJRUA6.0000900

[9] BIS IS 1893. (2002). Indian standard criteria for earthquake resistant design of structures (part 1): general provisions and buildings (fifth revision). Bureau of Indian Standards, New Delhi.

[10] Boroujeni, A. R. K. (2013). Evaluation of various methods of FEMA356 compare to FEMA440. Journal of Civil Engineering and Construction Technology, 4(2), 51-55. http://www.academicjournals.org/JCECT. DOI: 10.5897/JCECT12.082

[11] Chaudhary, S., & Choudhury, S. (2022). Performance-Based Seismic Design: A Review. In: Fonseca de Oliveira Correia, J.A., Choudhury, S., Dutta, S. (eds) Advances in Structural Mechanics and Applications. ASMA 2021. Structural Integrity, vol 27. Springer, Cham. https://doi.org/10.1007/978-3-031-04793-0_31

[12] Couto, R., Sousa, I., Bento, R., & Castro, J. M. (2022). Seismic vulnerability assessment of RC structures: research and practice at building level. In T. Ferreira & H. Rodrigues (Eds.), Seismic Vulnerability Assessment of Civil Engineering Structures At Multiple Scales (pp. 31-84). Woodhead Publishing. https://doi.org/10.1016/B978-0-12-824071-7.00001-9

[13] De Luca, F., & Verderame, G. M. (2015). Seismic Vulnerability Assessment: Reinforced Concrete Structures. In: Beer, M., Kougioumtzoglou, I.A., Patelli, E., Au, S.K. (eds) Encyclopedia of Earthquake Engineering. Springer, Berlin, Heidelberg. https://doi.org/10.1007/978-3-642-35344-4_252

[14] FEMA 273. (1996). NEHRP guidelines for the seismic rehabilitation of buildings. Washington (DC): Federal Emergency Management Agency.

[15] FEMA 356. (2000). Pre-standard and commentary for the seismic rehabilitation of buildings. Washington (DC): Federal Emergency Management Agency.

[16] FEMA 445. (2006). Next generation performance-based seismic design guidelines: program plan for new and existing buildings. Federal Emergency Management Agency, Washington (DC).

[17] Ghobarah, A. (2001). Performance-based design in earthquake engineering: state of development. Engineering Structures, 23, 878–884. https://doi.org/10.1016/S0141-0296(01)00036-0

[18] IS 13920. (1993). Ductile detailing of reinforced concrete structures subjected to seismic force-code of practice. Bureau of Indian standards, New Delhi.

[19] IS 456. (2000). Indian standard plain and reinforced concrete – code of practice (fourth revision). Bureau of Indian standards, New Delhi.

[20] IS 875. (1987). Code of practice for design loads (other than earthquake) for buildings and structures: part 1 dead loads. Bureau of Indian standards, New Delhi.

[21] IS 875. (1987). Code of practice for design loads (other than earthquake) for buildings and structures: part 2 imposed loads. Bureau of Indian standards, New Delhi.

[22] Jain, S.K. (2016). Earthquake Resistant Design of Structures (Revised Edition). Journal of Structural Engineering, 42 (3), 123-135. DOI: 10.1016/j.jstructeng.2016.03.001

[23] Jia, H., Song, Y., Chen, X., Liu, S., & Zhang, B. (2022). Seismic Performance Evaluation of a High-Rise Building with Structural Irregularities. Buildings, 12(9), 1484. https://doi.org/10.3390/buildings12091484

[24] Kuria, K.K., & Kegyes-Brassai, O.K. (2024). Pushover Analysis in Seismic Engineering: A Detailed Chronology and Review of Techniques for Structural Assessment. Applied Sciences, 14(1), 151. https://doi.org/10.3390/app14010151

[25] Mihai, Mihaită. (2015). A theoretical review of the damage indices used to model the dynamic behavior of reinforced concrete structures. Bulletin

 DOI : 10.35291/2454-9150.2024.0358

of Polytechnical Institute Iasi Construction and Architecture Section, 63(2), 109–119.

[26] Moehle, J. P. (2006). Seismic analysis, design, and review for tall buildings. The Structural Design of Tall and Special Buildings, 15(5), 495–513. https://doi.org/10.1002/tal.378

[27] Mokashi, V.M., Jadhav, H.S. Progressive collapse analysis and seismic performance of irregular RC structures: a probabilistic approach. Asian J Civ Eng 25, 4911–4921 (2024). https://doi.org/10.1007/s42107-024-01088-8

[28] Mondal, A., Ghosh, S., & Reddy, G. R. (2013). Performance-based evaluation of the response reduction factor for ductile RC frames. Engineering Structures, 56, 1808–1819. https://doi.org/10.1016/j.engstruct.2013.07.038

[29] Padalu, P.K.V.R., & Surana, M. (2024). An Overview of Performance-Based Seismic Design Framework for Reinforced Concrete Frame Buildings. Iran J Sci Technol Trans Civ Eng, 48, 635–667. https://doi.org/10.1007/s40996-023-01217-4

[30] Performance-Based Seismic Design for Tall Buildings by the Council on Tall Buildings and Urban Habitat (CTBUH). (2017). https://doi.org/10.1007/s40996-023-01217-4

[31] Powell, G H., & Allahabadi, R. (1988). Seismic damage prediction by deterministic methods: concept and procedure. Earthquake Engineering and Structural Dynamics, 16(5), 719–734.

[32] Shojaei, F., & Behnam, B. (2017). Seismic vulnerability assessment of low-rise irregular reinforced concrete structures using cumulative damage index. Advances in Concrete Construction, 5(4), 407-422. https://doi.org/10.12989/acc.2017.5.4.407

[33] Siva, N. E., Abraham, N. M., & Anitha, S. D. (2019). Analysis of irregular structures under earthquake loads. Procedia Structural Integrity, 14, 806-819. https://doi.org/10.1016/j.prostr.2019.07.059

[34] Soni, D. P., & Mistry, B. B. (2006). Qualitative review on seismic response of vertically irregular building frames. ISET Journal of Earthquake Technology, Technical Note, 43(4), 121-132.

[35] Valmundsson, E. V., & Nau, J. M. (1997). Seismic response of building frames with vertical structural irregularities. Journal of Structural Engineering, 123(1), 30–41. https://doi.org/10.1061/(ASCE)0733-9445(1997)123:1(30)

[36] Wilson, E. L., & Habibullah, A. (2000). SAP 2000/NL-push version 17 software, computer and structures, Inc, Berkeley, CA, USA.

[37] Zameeruddin, M., & Sangle, K. K. (2016). Review on recent developments in performance-based seismic design of reinforced concrete structures. Structures, 6, 119–133. https://doi.org/10.1016/j.istruct.2016.03.001

[38] Zameeruddin, M., & Sangle, K. K. (2017a). Seismic performance evaluation of reinforced concrete frames subjected to seismic loads. Journal of the Institution of Engineers (India): Series A, 98, 177–183. https://doi.org/10.1007/s40030-017-0196-0

[39] Zameeruddin, M., & Sangle, K. K. (2017b). Seismic damage assessment of reinforced concrete structure using nonlinear static analyses. KSCE Journal of Civil Engineering, 21(4), 1319–1330. https://doi.org/10.1007/s12205-016-0541-2

[40] Zameeruddin, M., & Sangle, K. K. (2017c). Energy-based damage assessment of RCMRFs using pushover. Asian Journal of Civil Engineering (BHRC), 18(7), 1077–1093.

[41] Zameeruddin, M., & Sangle, K. K. (2021). Performance-based seismic assessment of reinforced concrete frames. Journal of King Saud University Engineering Sciences, 33(3), 153-165. https://doi.org/10.1016/j.jksues.2020.04.005

[42] Zameeruddin, M., & Sangle, K. K. (In press). Damage assessment of reinforced concrete moment resisting frames using performance-based seismic evaluation procedures. Journal of King Saud University Engineering Sciences. https://doi.org/10.1016/j.jksues.2020.04.010

 DOI : 10.35291/2454-9150.2024.0358